BULLETIN OF THE POLISH ACADEMY OF SCIENCES
TECHNICAL SCIENCES, Vol. 63, No. 1, 2015
DOI: 10.1515/bpasts-2015-0030

Deliberations about three-phase PLL technologies applied to a grid control of the renewable power system

L. LIU[1,2] and C. LIU[2*]

[1] College of Electrical and Power Engineering, Taiyuan University of Technology,
79 Yingze West Street, Wanbolin District, Taiyuan, People's Republic of China
[2] College of Electronic and Information Engineering, Taiyuan University of Science & Technology,
66 Waliu Road, Wanbolin District, Taiyuan, People's Republic of China

Abstract. An efficient phase locked loop (PLL) method is very important to improve the grid-connected efficiency and the locked speed of frequency, phase, and voltage. However, most of literatures only introduce one PLL or one modified PLL method. There are many grid faults due to the grid connection to the renewable power generating system. A comparison and analysis is very important to select the most effective PLL technology for the grid-connected control of the renewable power system. Three PLL technologies are compared at different grid faults, such as single phase voltage drop, two phase voltage drop, frequency deviation, and voltage distortion. Simulation results indicated that different PLL methods have different locked performances at different grid faults.

Key words: Grid-connected, Phase locked loop (PLL), SSRF-PL,; DDSRF-PLL, E-PLL.

1. Introduction

The development of modern society needs enough power supply, and billions of tons of fossil fuel is consumed to provide enough electric power to meet the demand of ordinary people, industry, and agriculture, etc. Enough energy supply has become an engine of national development no matter a developed country or a developing country, however, astronomical energy consumption has brings a series of environmental problems such as greenhouse gas emissions, environment pollution, acid rain, and sea level rise, etc, which has affect the sustainable development of human being and the survival of millions of people. So the traditional energy structure in the 20th century must be rejected, and the low-carbon economy mode and the low-carbon lifestyle in 21st century for world countries are very important, it is possible to realize the sustainable development of the world [1]. Fortunately, there are some experts have realized the important of renewable energy such as solar energy, wind energy, biomass energy, tidal energy, and geothermal energy, and so on. The application and utilization of renewable energy has come in the rapid develop stage in the global scale, especially, the wind and solar energy has a share of the total energy structure of the world [2–4], the renewable. Normally, a power system can be divided into two classes: a stand-alone and a grid-connected. The generating capacity of the stand-alone renewable generating system is small with kW, which has been used in some domains. For example, some industry equipments located in remote areas which apart from the power grid, such as the communication base station, the island power system, and the radar station, and so on. The generating system which uses the renewable sources can afford steady electricity supply [5]. The generating capacity of a grid-connected system is generally big with MW. With the ever-increasing of installed capacity of a renewable generating system, the grid-connected technique becomes more and more important.

Many PLL techniques have been presented over the recent years. In synchronous reference frame based PLL based systems, the phase angle estimation is adaptively updated by a closed loop mechanism whose objective is to track the actual frequency and phase angle [6]. The three-phase grid-connected converter is widely used in renewable and electric power system applications. Traditionally, control of the three-phase grid-connected converter is based on the standard decoupled d–q vector control mechanism [7]. Many international application examples have been introduced in some literatures [8]. Furthermore, the grid-connected of renewable power system can be affected by the weather, grid faults, personal factors, etc. And the renewable energy density is very small, i.e., the energy densities of solar or wind energy have a share of about 1/1000 of the water energy at the same speed. Furthermore, there are some grid faults such as single-phase voltage drop, two phase voltage drop, frequency deviation, and voltage distortion. Some PLL technologies have been described in many literatures, such as Single Synchronous Reference Frame Phase Locked Loop (SSRF-PLL), Decoupled Double Synchronous Reference Frame Phase Locked Loop (DDSRF-PLL), and Enhanced Phase Locked Loop (E-PLL). In this paper, different grid faults of three PLL technologies base on d-q vector are analyzed to gain the most effective PLL technology to certify the safety of the grid-connected of renewable power system.

2. SSRF-PLL and DDSRF-PLL and E-PLL

The accurate phase angle and frequency for a grid-connected renewable generating system is very important to realize the power factor correction, active/reactive power control and gain

*e-mail: llqd2004@163.com

the utility voltage of grid. However, the work is very difficult since the voltage or current reference is synchronized with the phase of the utility voltage. There are some PLL technologies that have been described in many literatures such as SSRF-PLL, DDSRF-PLL, and E-PLL. In order to gain the output performance at different grid faults, three PLL methods are simple introduced in this section.

The SSRF-PLL methods can adaptively track the actual frequency and phase angle by using a closed loop. Their structure is very simple. The modelling of SSRF-PLL is introduced as follows:

The three phase voltages V_a, V_b, V_c are expressed as Eq. (1).

$$\begin{bmatrix} V_a \\ V_b \\ V_c \end{bmatrix} = \begin{bmatrix} V_m \cos\theta \\ V_m \cos(\theta - 2\pi/3) \\ V_m \cos(\theta + 2\pi/3) \end{bmatrix}. \tag{1}$$

The three-dimensional coordinates are transformed into the stationary reference frame signals V_α and V_β as it is expressed in (2). Where, $V_\gamma = 0$ because of V_a, V_b, V_c are symmetrical.

The stationary reference frame signals are transformed to the rotating reference frame signals V_d and V_q as expressed (3).

$$\begin{bmatrix} V_\alpha \\ V_\beta \\ V_\gamma \end{bmatrix} = \frac{2}{3} \begin{bmatrix} 1 & -1/2 & -1/2 \\ 0 & \sqrt{3}/2 & -\sqrt{3}/2 \\ 1/2 & 1/2 & 1/2 \end{bmatrix} \begin{bmatrix} V_a \\ V_b \\ V_c \end{bmatrix}, \tag{2}$$

$$\begin{bmatrix} V_d \\ V_q \end{bmatrix} = \begin{bmatrix} \cos\theta' & \sin\theta' \\ -\sin\theta' & \cos\theta' \end{bmatrix} \begin{bmatrix} V_\alpha \\ V_\beta \end{bmatrix}, \tag{3}$$

where $\theta' = \omega' t$, and ω' is the angular frequency of the rotating d-q frame, and t is the time. θ is the actual phase and θ' is the accurate estimate. When $\theta' - \theta = 0$, the PLL gets locked to the utility voltage. V_m is the magnitude of voltage. And a proportional-integral (PI) controller is used in V_q. The model diagram of SSRF-PLL can be seen from Fig. 1. PI controller is equivalent to a loop filter, and K_p and K_i are the parameters of PI, which are 10 and 802 in this paper, respectively.

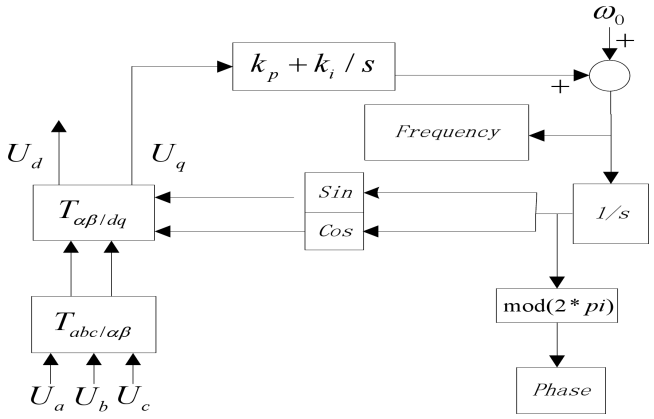

Fig. 1. Model diagram of SSRF-SPLL

In DDSRF-PLL, the three phase voltages V_a, V_b, V_c are expressed as Eq. (4) using symmetrical component method.

The three-dimensional coordinates are transformed into the stationary reference frame signals V_α and V_β as it is expressed in (2).

Here, $V_s = V_s^{+1} + V_s^{-1} + V_s^0$. Moreover, the V_s^{+1}, V_s^{-1}, and V_s^0 are the positive-sequence, negative sequence, and zero-sequence components of grid voltage vector V_s, respectively. And the ϕ^{+1}, ϕ^{-1}, and ϕ^0 are the positive sequence, negative sequence, and zero-sequence starting phase angle of fundamental voltage.

$$\begin{aligned} \begin{bmatrix} V_a \\ V_b \\ V_c \end{bmatrix} &= V_s^{+1} \begin{bmatrix} \cos(\omega t + \phi^{+1}) \\ \cos(\omega t - 120^\circ + \phi^{+1}) \\ \cos(\omega t + 120^\circ + \phi^{+1}) \end{bmatrix} \\ &+ V_s^{-1} \begin{bmatrix} \cos(-\omega t + \phi^{-1}) \\ \cos(-\omega t - 120^\circ + \phi^{-1}) \\ \cos(-\omega t + 120^\circ + \phi^{-1}) \end{bmatrix} \\ &+ V_s^0 \begin{bmatrix} \cos(\omega t + \phi^0) \\ \cos(\omega t + \phi^0) \\ \cos(\omega t + \phi^0) \end{bmatrix}. \end{aligned} \tag{4}$$

Equation (4) can be simplified as (5) due to the zero-sequence component $V_s^0 = 0$ after transformation.

$$\begin{aligned} \begin{bmatrix} V_\alpha \\ V_\beta \end{bmatrix} &= V_s^{+1} \begin{bmatrix} \cos(\omega t + \phi^{+1}) \\ \sin(\omega t + \phi^{+1}) \end{bmatrix} \\ &+ V_s^{-1} \begin{bmatrix} \cos(-\omega t + \phi^{-1}) \\ \sin(-\omega t + \phi^{-1}) \end{bmatrix}. \end{aligned} \tag{5}$$

The grid voltage vector V_s can resolves into V_s^{+1} (rotates with angular frequency ω) and V_s^{-1} (rotates with angular frequency $-\omega$). The stationary reference frame signals are transformed to two rotating reference frame signals: V_d^{+1} and V_q^{+1}, and V_d^{-1} and V_q^{-1}, which are expressed as (6) and (7)

$$\begin{bmatrix} V_d^{+1} \\ V_q^{+1} \end{bmatrix} = \begin{bmatrix} \cos\theta' & \sin\theta' \\ -\sin\theta' & \cos\theta' \end{bmatrix} \begin{bmatrix} V_\alpha \\ V_\beta \end{bmatrix}, \tag{6}$$

$$\begin{bmatrix} V_d^{-1} \\ V_q^{-1} \end{bmatrix} = \begin{bmatrix} \cos\theta' & -\sin\theta' \\ \sin\theta' & \cos\theta' \end{bmatrix} \begin{bmatrix} V_\alpha \\ V_\beta \end{bmatrix}. \tag{7}$$

If $\theta' - \theta \approx 0$, V_s^{+1} will approach the axis d^{+1} of positive sequence component. Equations (6) and (7) can be expressed as (8) and (9) using the (5)

$$\begin{aligned} \begin{bmatrix} V_d^{+1} \\ V_q^{+1} \end{bmatrix} &\approx \begin{bmatrix} V_d^{+1*} \\ V_q^{+1*} \end{bmatrix} \\ &+ \begin{bmatrix} \overline{V}_d^{-1} \cos(2\theta') + \overline{V}_q^{-1} \sin(2\theta') \\ \overline{-V}_d^{-1} \sin(2\theta') + \overline{V}_q^{-1} \cos(2\theta') \end{bmatrix}, \end{aligned} \tag{8}$$

$$\begin{aligned} \begin{bmatrix} V_d^{-1} \\ V_q^{-1} \end{bmatrix} &\approx \begin{bmatrix} V_d^{-1*} \\ V_q^{-1*} \end{bmatrix} \\ &+ \begin{bmatrix} \overline{V}_d^{+1} \cos(2\theta') - \overline{V}_q^{+1} \sin(2\theta') \\ \overline{V}_d^{+1} \sin(2\theta') + \overline{V}_q^{+1} \cos(2\theta') \end{bmatrix}. \end{aligned} \tag{9}$$

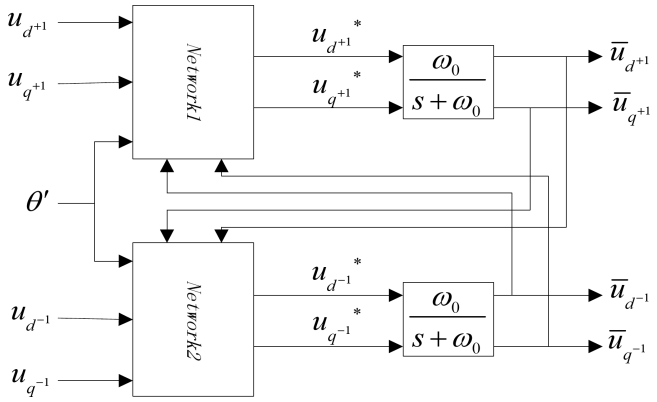

Fig. 2. Decoupling network diagram

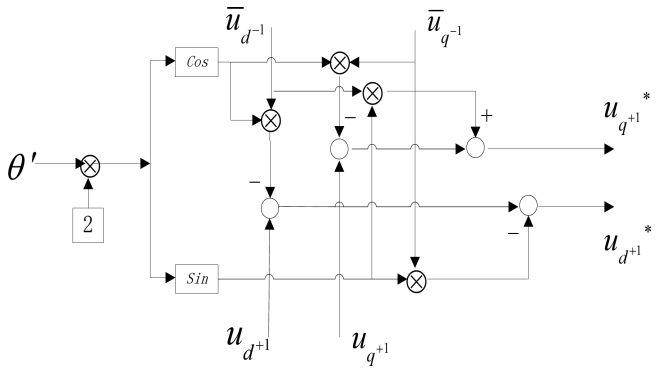

Fig. 3. Schematic diagram of Network1

In order to eliminate the perturbation of alternating (AC) component with negative direction since the V_d^{+1} and V_d^{+1} include the negative sequence AC components and the V_d^{-1} and V_q^{-1} include the positive-sequence AC components which is bad to lock the voltage phase. So the V_d^{+1*} and V_d^{+1*} are used to replace the V_d^{+1} and V_d^{+1} to eliminate the perturbation of AC components. Equations (8) and (9) can be constituted a network block diagram as shown in Fig. 2. Here, the schematic diagram of network1 can be seen from Fig. 3. Network2 is similar with network1 by replacing the positive and negative sequence component in Network1.

It is difficult to lock the voltage phase for SSRF-PLL at unstable voltage due to the big effect of negative sequence voltage of three-phase voltage. In E-PLL, to eliminate the effect and improve the capability of locked phase and locked frequency, the positive-sequence voltage is extract from three-phase voltage by using the transfer matrix (10).

$$\begin{bmatrix} V_a^{+1} \\ V_b^{+1} \\ V_c^{+1} \end{bmatrix} = \frac{1}{3} \begin{bmatrix} 1 & a & a^2 \\ a^2 & a & a \\ a & a^2 & 1 \end{bmatrix} \begin{bmatrix} V_a \\ V_b \\ V_c \end{bmatrix}. \tag{10}$$

Here, $a = -\frac{1}{2} \pm \frac{\sqrt{3}}{2} e^{i90}$.

Then Eq. (10) can be given by

$$\begin{bmatrix} V_a^{+1} \\ V_b^{+1} \\ V_c^{+1} \end{bmatrix} = \begin{bmatrix} \frac{1}{3}V_a - \frac{1}{6}(V_b + V_c) - \frac{1}{2\sqrt{3}} C_{90}(V_b - V_c) \\ \frac{1}{3}V_b - \frac{1}{6}(V_a + V_c) - \frac{1}{2\sqrt{3}} C_{90}(V_c - V_a) \\ \frac{1}{3}V_c - \frac{1}{6}(V_a + V_b) - \frac{1}{2\sqrt{3}} C_{90}(V_a - V_b) \end{bmatrix}. \tag{11}$$

Here, $V_b^{+1} = -V_a^{+1} - V_c^{+1}$, and C_{90} is the clockwise phase 90°.

The output voltage of PLL and positive AC component can be gained using the E-PLL as can be seen from Fig. 4. The E-PLL consists of the phase detector loop filter and voltage-controlled oscillator, etc. The three-phase voltages are filtered to approach the fundamental wave of three-phase equilibrium voltage to improve the anti-interference capacity of PLL. When gained the V_a^{+1}, V_b^{+1}, and V_c^{+1}, the locked phase algorithm is similar with SSRF-PLL. Here, y and $y90$ are the locked phase voltage and orthogonal vector.

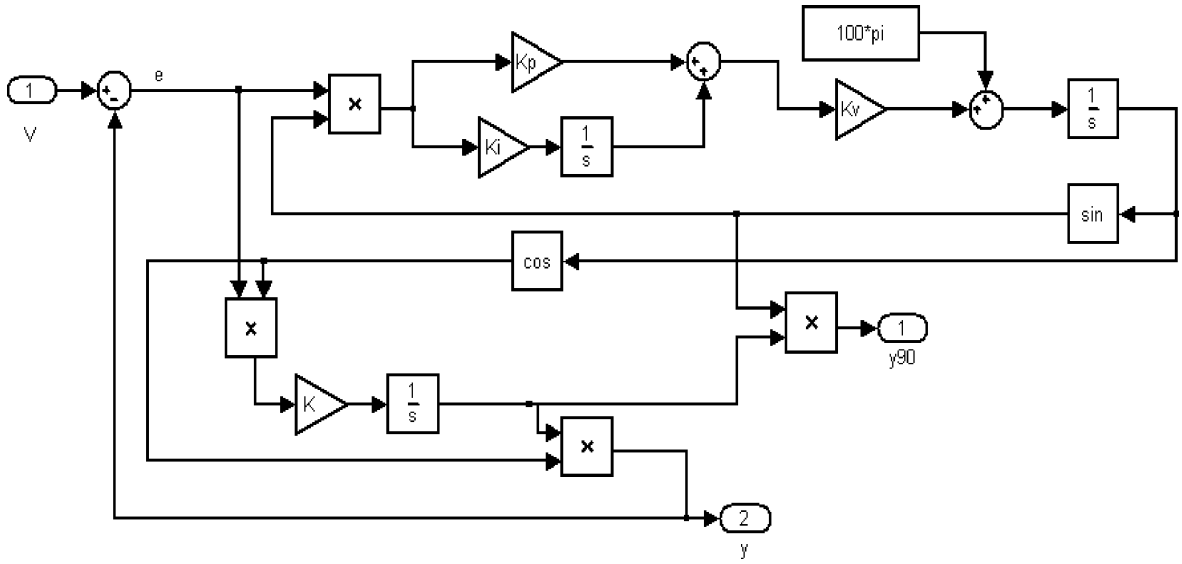

Fig. 4. Diagram of EPLL

3. Simulation results at different voltage faults

To clarify the advantages and disadvantages of three PLL technologies, different word conditions are considered in this section such as the ideal situation, single-phase voltage drop, two phase voltage drop, frequency discontinuity, and voltage distortion.

As shown in Fig. 5, the SSRF-SPLL can track the frequency and phase and voltage of grid, which has high precision and rapid response speed under ideal conditions. The tracking performance using DDSRF-PLL is worse than that of SSRF-PLL, and the tracking characteristics of E-PLL are the worst to compare with that of SSRF-PLL and DDSRF-PLL. For example, the frequency locked speed using E-PLL is very slow compare with other two methods.

Single phase voltage drop is normally grid fault, and the three phase output voltage is shown in Fig. 6a. The output voltage of A phase is 0 volt from 0.05 s, that is, the single phase voltage drop causes in 0.05 second. The tracking performance of frequency and phase and voltage locked at Single phase voltage drop can be seen from Fig. 6b and Fig. 6c and Fig. 6d.

The E-PLL has the best tracking performance at this situation, and the SSRF-PLL has the worst tracking performance, i.e., the frequency locked is very rapid using E-PLL and there are small oscillation. At the same conditions, the oscillations are big and the tracking speeds are slow using SSRF-PLL and DDSRF-PLL. Furthermore, the phase locked performance using E-PLL is the more excellent than that of SSRF-PLL and DDSRF-PLL. Moreover, the voltage locked performance is excellent using E-PLL which can accurately estimate the A phase recovery voltage as compare with that of SSRF-PLL and DDSRF-PLL. Where, Fig. 6e is the partial enlarged drawing of Fig. 6d.

The three phase output voltage at two phase voltage drop from 0.05 s is shown in Fig. 7a. There are the largest frequency oscillation using DDSRF-PLL as shown in Fig. 7b, and the largest phase and voltage excursion using E-PLL as can be seen from Figs. 7c and 7 d. Here, the two phase voltage drop causes in 0.05 second.

Figure 8 a shows the frequency deviation of three phase voltage. Here, the deviation change is from 50 Hz to 40 Hz. The SSRF-PLL and DDSRF-PLL have the excellent tracking performances as compare with E-PLL, i.e., the locked speed of frequency using E-PLL is slower than that of SSRF-PLL and DDSRF-PLL. And the phase and voltage using E-PLL cause big deviation as compare with other two methods.

In Fig. 9, the voltage distortion is described. The voltage and frequency cause the change of three phase output voltage at this condition. Figure 9a shows the distortion of three phase output voltage, and the distortion causes in 0.05 s. The locked performance of E-PLL is the best as shown in Fig. 9b and Fig. 9c and Fig. 9d.

As mention above, the locked performances of SSRF-PLL under ideal and two phase voltage drop and frequency deviation are more excellent than that of DDSRF-PLL and E-PLL. However, the locked performances of E-PLL at single phase voltage drop and voltage distortion are the best as compare with that of SSRF-PLL and DDSRF-PLL. It is very important to select different PLL technologies at different grid faults.

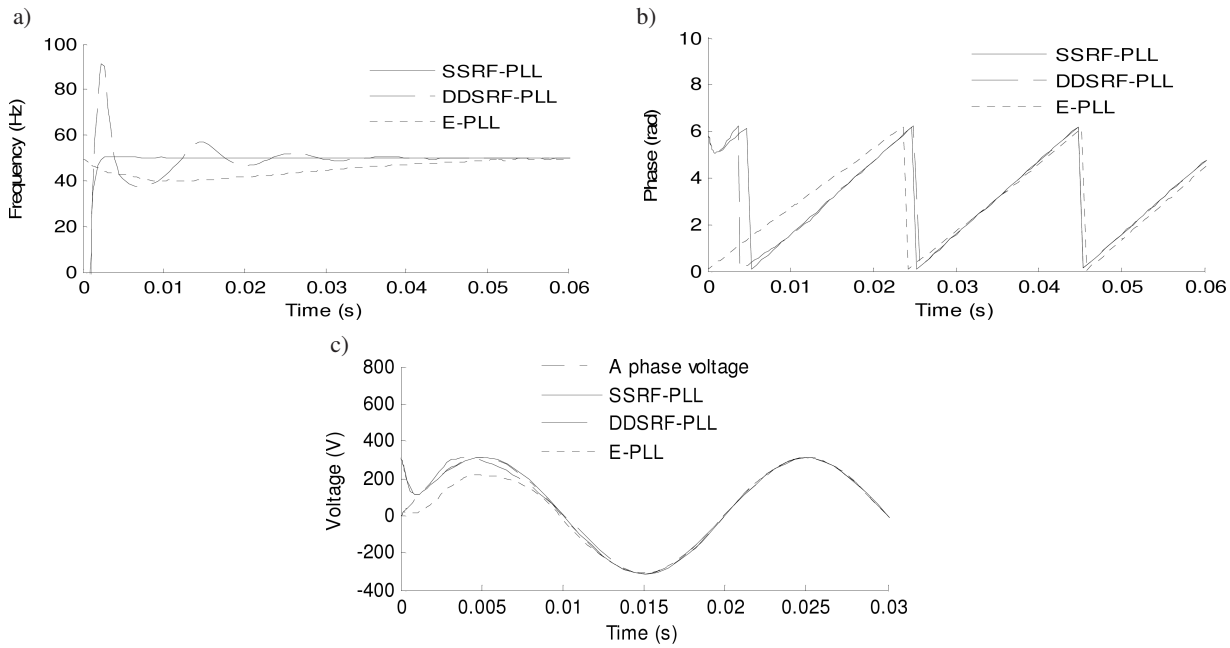

Fig. 5. Frequency and phase and voltage locked of three type PLL technologies under ideal conditions

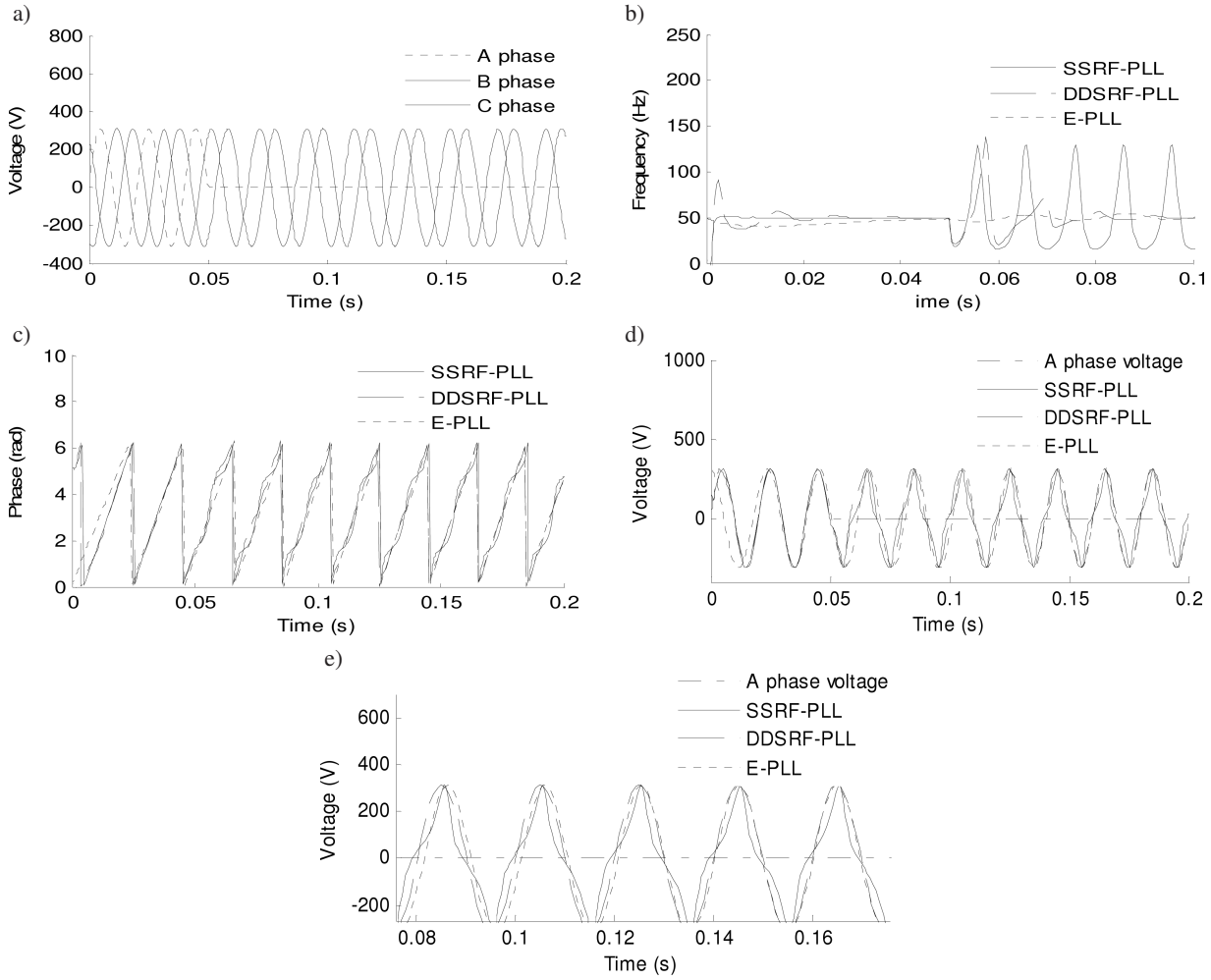

Fig. 6. Three-phase output voltage, frequency and phase and voltage locked of three type PLL technologies at single phase voltage drop

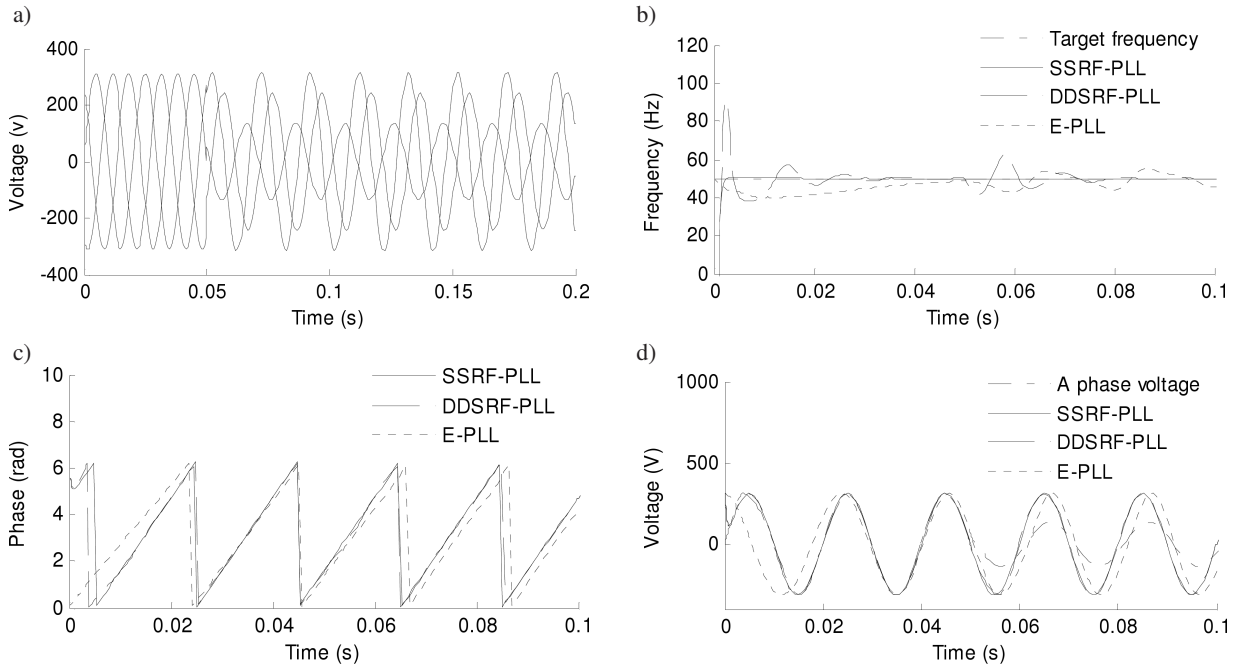

Fig. 7. Frequency and phase and voltage locked of three PLL technologies at two phase voltage drop

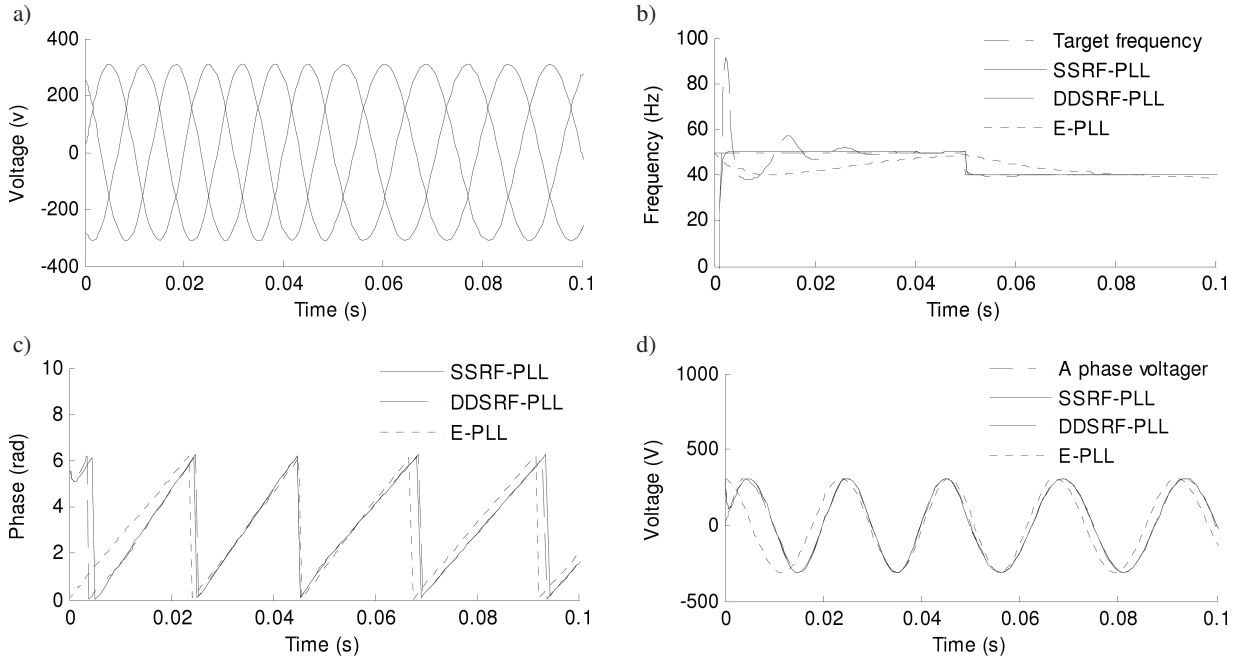

Fig. 8. Frequency and phase and voltage locked of three PLL technologies at frequency deviation

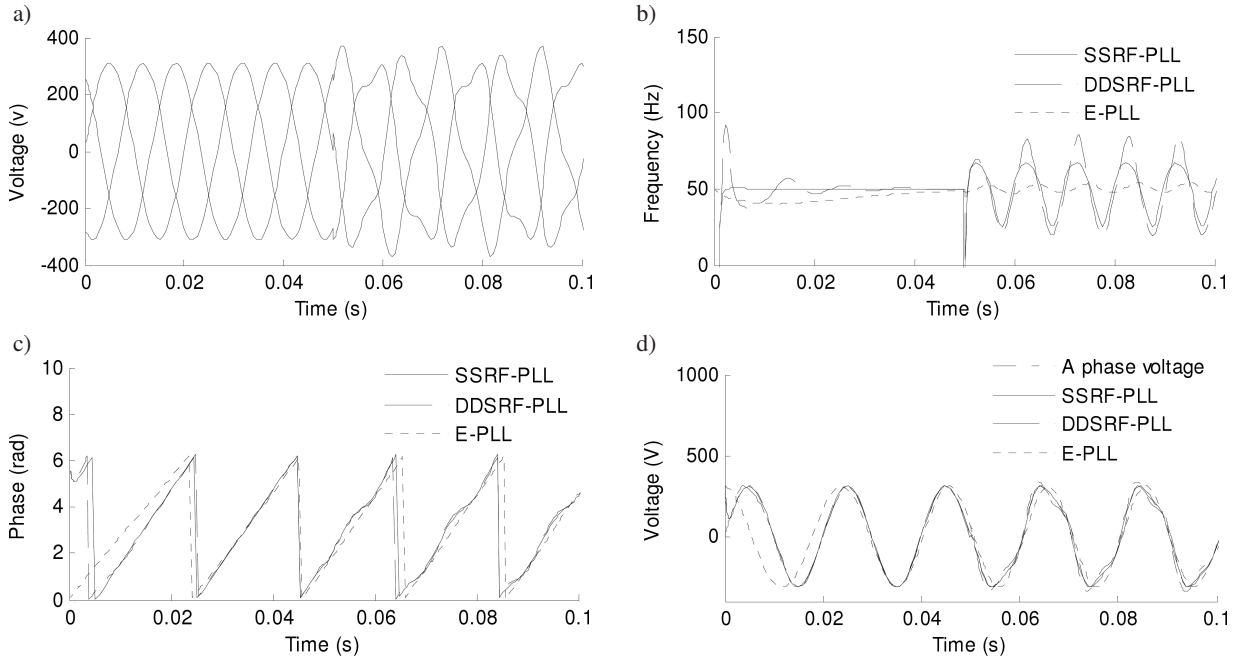

Fig. 9. Comparison of frequency and voltage locked at voltage distortion

4. Conclusions

There are many PLL technologies which have been introduced in literature, such as SSRF-PLL, DDSRF-PLL, and E-PLL, etc. It is very important, however, to select the most effective PLL under different grid faults conditions. In this paper, in order to gain the most effective PLL for the grid-connected of the renewable power system, above three PLL technologies are compared at single phase voltage drop, two phase voltage, frequency deviation, and voltage distortion. Simulation results depict that the SSRF-PLL has the most excellent performances at ideal, two phase voltage drop, and frequency deviation and the E-PLL has the most excellent performances at single phase voltage drop and voltage distortion. In a conclusion, the different PLL can be used in different grid faults, and the most effective PLL can be selected to reply the different grid faults to improve the grid-connected performance and locked speed.

Acknowledgements. Funding for this work was provided by the China Postdoctoral Science Foundation (NO: 2014T70234, 2013M530895) and Funding for this work was provided by the China Postdoctoral Science Foundation (NO: 2014T70234, 2013M530895) and Soft Science Research Program of Shanxi province (NO: 2014041021-3).

REFERENCES

[1] L.Q. Liu, C.X. Liu, and Z.Y. Sun, "A survey of China's low-carbon application practice -opportunity goes with challenge", *Renewable and Sustainable Energy Reviews* 15 (6), 2895–2903 (2011a).

[2] L.Q. Liu, C.X. Liu, Z.Y. Sun, and R.C. Han, "The development and application practice of neglected tidal energy in China", *Renewable and Sustainable Energy Reviews* 15 (2), 1089–1097 (2011).

[3] L.Q. Liu and Z.X. Wang, "The development and application practice of wind–solar energy hybrid generation systems in China", *Renewable and Sustainable Energy Reviews* 13 (6–7), 1504–1512 (2009).

[4] L.Q. Liu, Z.X. Wang, H.Q. Zhang, and Y.C. Xue, "Solar energy development in China-A review", *Renewable and Sustainable Energy Reviews* 14 (1), 301–311 (2010).

[5] L.Q. Liu and C.X. Liu, "Techno-economic analysis of off-grid renewable energy power station a case study", *Przeglad Elektrotechniczny (Electrical Review)* 88 (7a), 94–98 (2012).

[6] B. Indu Rani, C.K. Aravind, G. Saravana Ilango, and C. Nagamani, "A three phase PLL with a dynamic feed forward frequency estimator for synchronization of grid connected converters under wide frequency variations", *Int. J. Electrical Power and Energy Systems* 41 (1), 63–70 (2012).

[7] S. Li, T.A. Haskew, Y.K. Hong, and L. Xu , "Direct-current vector control of three-phase grid-connected rectifier–inverter", *Electric Power Systems Research* 81 (2), 357–366 (2011).

[8] J.H. So, Y.S. Jung, G.J. Yu, J.Y. Choi, and J.H. Choi, "Performance results and analysis of 3 kW grid-connected PV systems", *Renewable Energy* 32 (11), 1858–1872 (2007).